

3D-FDTD Computation of Lightning Electromagnetic Fields in the Presence of a Mountain and a River

Kaddour Arzag
Dept. of Electrotechnics
UTMS of Saida
LDEE Lab. USTO-MB
Saida, Algeria
ar_kado2006@yahoo.fr

Zin-Eddine Azzouz
Dept. of Automatic and Control
USTO-MB of Oran
LDEE Lab. USTO-MB
Oran, Algeria
zinazzouz@yahoo.fr

Yoshihiro Baba
Dept. of Electrical Engineering
Doshisha University
Kyoto, Japan
ybaba@mail.doshisha.ac.jp

Abstract—In this paper, we studied the influence of the presence of a wide river on electromagnetic fields generated by lightning strikes to a tall tower located on a high mountain, using the three-dimensional finite-difference time-domain method. In the computations, the lightning channel and the tower are represented by the transmission line model extended to include a tall strike object. Electromagnetic fields are computed at different points located in the river and above the ground. It is shown that the peak value and the electromagnetic field waveforms, computed at the considered observation points, are significantly affected by the presence of the river.

Keywords—Lightning electromagnetic fields; 3D finite difference time domain (3D-FDTD) method; tower; mountain; river.

I. INTRODUCTION

In lightning electromagnetic pulse (LEMP) propagation studies, it is quite important to take into account the influence of tall structures such as towers and that of mountains and rivers. There are many works on the computation of LEMP associated with lightning strikes to tall objects [1-15]. Also, LEMPs generated by a lightning strike to a top of a mountain have been evaluated [16]-[20], and the case of lightning strikes to a tower located on a mountain has been analyzed [21]. Furthermore, the effect of the presence of a river on the lightning induced current has been studied [22]. Note that LEMPs associated with lightning strikes are frequently evaluated [23] using electromagnetic computation methods such as the finite-difference time-domain (FDTD) method [24], the method of moments [25], and the finite element method (FEM) [26].

In this paper, we evaluate the influence of the presence of a river on electromagnetic fields produced by lightning strikes to the top of a tower located on a trapezoidal mountain. This evaluation is carried out by the implementation of the three-dimensional finite-difference time-domain (3D-FDTD) method [23] and the uniaxial perfectly matched layers (UPML) boundary conditions based on the Taflovie formulation [27-29]. The lightning current is represented with the transmission-line (TL) model [30] extended to include a tall strike object [2]. Indeed, the aim of this evaluation is to quantify the electromagnetic field components which are the principal cause of the induced disturbances on the nearby overhead lines as

well as the buried power or communication cables which can be on or under the water layer of the river.

This paper is structured as follows: Section II presents the methodology used for the lightning electromagnetic fields calculation. Section III is devoted to presentation of the obtained simulation results. A discussion and a comparison between the electromagnetic field waveforms, calculated in the case of presence and absence of the river are also done. Finally in Section IV, general conclusions are given.

II. MODELING AND METHODOLOGY

A. Configuration

Figure 1 shows the geometry of problem treated. The working space is divided into two zones. The first one represents the air and the second zone represents the soil. As shown in Fig.1 (a), in the soil zone, there is a trapezoidal mountain having a height of 300 m, an inclination angle of 30°, a base side of 1122 m, and a top side of 102 m. Also, this same area includes a river having a width of 51 m and a water layer with a depth of 5 m below which there is a ground layer with a depth of 95 m. The flat ground appearing in this figure is characterized by a thickness of 110 m. The surface of the river is located 10 m below the ground surface. A 100 m long strike tower is located at the center of the top surface of the mountain at distances of 150 m and 561 m from the lateral sides of the working space. The vertical lightning channel has a length of 1100 m. Electromagnetic field observation points are denoted as Points A, B and C in Fig. 1. Point A is located 800 m horizontally away from the foot of the mountain and 10 m above the flat ground. Point B is located 519 m horizontally away from the foot of the mountain and 2 m under the water surface. Point C is located 519 m horizontally away from the foot of the mountain and 2 m under the water bottom (in the soil). Furthermore, the river is located at a horizontal distance of 493 m from the foot of the mountain, and at a horizontal distance of 559 m from the right side of the working space.

This system is accommodated in a working volume of 2125 m × 300 m × 1610 m. Except for the layer between the flat ground surface and the lower surface of the water at a depth of 15 m in the ground which is divided into rectangular parallelepiped cells of 5 m × 8.5 m × 0.5 m, the entire working

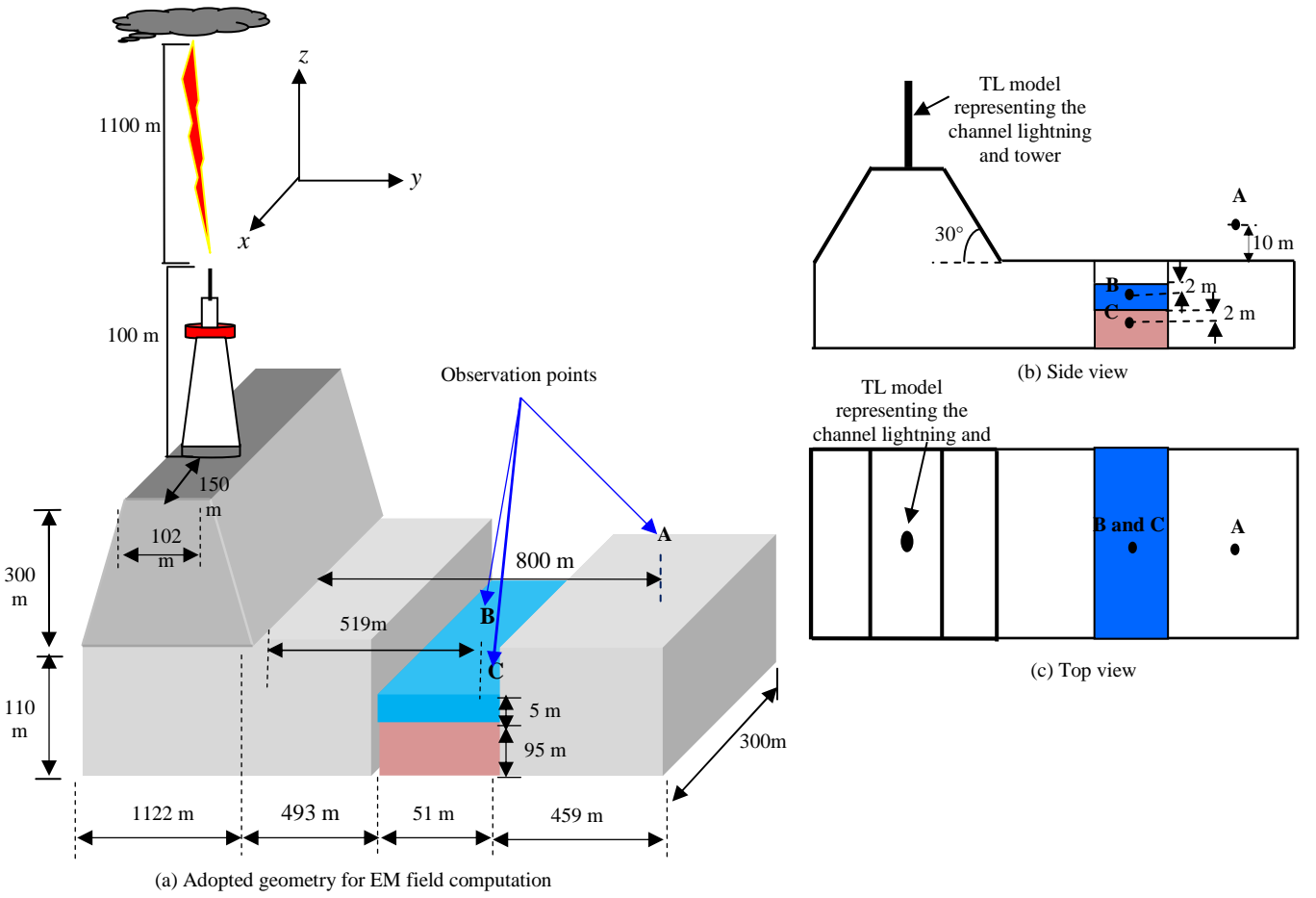


Fig.1. (a) Adopted geometry for LEMP computation, (b) and (c) positions of the transmission line and the observation points, (b) side view and (c) top

space is divided uniformly into rectangular parallelepiped cells of $5 \text{ m} \times 8.5 \text{ m} \times 5 \text{ m}$, which is composed of about 5×10^6 cells. These cells dimensions are chosen for having a steepness angle of 30° . Thus, for this reason, we added up the distances 493 m and 51 m which are calculated by multiplying the number of cells of each place with the length of the cell (8.5 m). The time increment is set to 0.75 ns, and the observation time is taken equal to 18 μs .

The water of river is characterized by a conductivity of 0.005 S/m and a relative permittivity of 30 [22]. The soil layer under the river has a conductivity value of 0.1 S/m and a permittivity of 10, and the ground other than the soil layer under the river has a conductivity value of 0.001 S/m and a permittivity of 10.

The uniaxial perfectly matched layer absorbing boundary condition [27] is applied to the six planes surrounding the working volume in order to suppress unwanted reflections.

The space-time distribution of the current along the lightning channel and along the tower is represented using the model [2], which is based on the TL model [30] of the lightning return stroke extended to include a tall strike object. The mathematical representation of these distributions is given as follows:

Along the strike tower:

$$I(z', t) = \frac{1 - \rho_{top}}{2} \sum_{n=0}^{\infty} \left[\rho_{bot}^n \rho_{top}^n I_{sc} \left(h, t - \frac{h - z'}{c} - \frac{2nh}{c} \right) + \rho_{bot}^{n+1} \rho_{top}^n I_{sc} \left(h, t - \frac{h + z'}{c} - \frac{2nh}{c} \right) \right] \quad (1-a)$$

$0 \leq z' \leq h$

Along the lightning channel:

$$I(z', t) = \frac{1 - \rho_{top}}{2} \left[I_{sc} \left(h, t - \frac{h - z'}{c} \right) + \sum_{n=1}^{\infty} \rho_{bot}^n \rho_{top}^{n-1} (1 + \rho_{top}) I_{sc} \left(h, t - \frac{h + z'}{v} - \frac{2nh}{c} \right) \right] \quad (1-b)$$

$z' \geq h$

Where n is an index of the successive reflections between the top and the bottom of the tower, c is the light speed ($3 \times 10^8 \text{ m/s}$), v the lightning current speed along the lightning channel ($v = 1.5 \times 10^8 \text{ m/s}$), I_{sc} is the lightning short-circuit current. The current reflection coefficient at the bottom of the tower (ρ_{bot}) and the current reflection coefficient at the top of the tower (ρ_{top}) are given by:

$$\rho_{bot} = \frac{Z_{tow} - Z_{gr}}{Z_{tow} + Z_{gr}} \quad (2)$$

$$\rho_{top} = \frac{Z_{tow} - Z_{ch}}{Z_{tow} + Z_{ch}} \quad (3)$$

Where Z_{ch} is the characteristic impedance of the lightning channel, Z_g is the grounding impedance, and Z_{tow} is the characteristic impedance of the tower. The values of the reflection coefficients are set to $\rho_{bot} = 1$ and $\rho_{top} = -0.5$ taken from reference [2].

The channel-base current (at the contact point between lightning and the top of the tower) used here has a peak of 12 kA and a rise time of 0.7 μ s. This current is represented with Heidler functions [31] as shown in Equation (4) and in Table I [28]:

$$i(0, t) = \frac{i_{01}}{n_1} \frac{(t/\tau_{11})^{n_1}}{1 + (t/\tau_{11})^{n_1}} \exp\left(\frac{-t}{\tau_{12}}\right) + \frac{i_{02}}{n_2} \frac{(t/\tau_{21})^{n_2}}{1 + (t/\tau_{21})^{n_2}} \exp\left(\frac{-t}{\tau_{22}}\right) \quad (4)$$

Where i_{01} and i_{02} are the current amplitudes, τ_{11} and τ_{12} are the front-time constants, and τ_{21} and τ_{22} are the decay time constants, and n_1 and n_2 are exponents.

$$\eta_1 = \left[-\left(\frac{\tau_{11}}{\tau_{12}}\right) \left(n_1 \cdot \frac{\tau_{12}}{\tau_{11}}\right)^{\frac{1}{n_1}} \right], \quad \eta_2 = \left[-\left(\frac{\tau_{21}}{\tau_{22}}\right) \left(n_2 \cdot \frac{\tau_{22}}{\tau_{21}}\right)^{\frac{1}{n_2}} \right]$$

TABLE I. CONSTANTS USED IN THE REPRESENTATION OF THE CHANNEL-BASE CURRENT

i_{01} (kA)	τ_{11} (μ s)	τ_{12} (μ s)	i_{02} (kA)	τ_{21} (μ s)	τ_{22} (μ s)	n_1	n_2
10.5	0.25	2.5	6.5	2.1	230	2	2

III. RESULTS AND ANALYSIS

A. Vertical electric field

Space and time variations of the vertical electric field E_z at Points A, B, and C in Fig. 1 are shown in this section. In order to show the influence of the presence of river, corresponding waveforms of E_z in the absence of river, where the 5-m deep and 0.005-S/m river, the 0.1-S/m high conducting soil layer below the river, and the 5-m thick air layer above the river are replaced by a uniform 0.001-S/m soil, are shown.

Fig. 2(a) shows waveforms of E_z at Point A in both the presence and absence of river. It follows from Fig. 2 (a) that the presence of the 51-m wide and 5-m deep dip of the ground due to the river decreases E_z located beyond the river.

Fig. 2 (b-1) shows the waveform of E_z at Point B (at a depth of 7 m in the 0.001-S/m soil) in the absence of river, and Fig. 2 (b-2) shows that in the presence of river (at a depth of 2 m from the surface of 0.005-S/m river water). It appears that E_z at a depth of 7 m in the 0.001-S/m soil is significantly more attenuated than that at a depth of 2 m in the 0.005-S/m water.

Fig. 2 (c-1) shows the waveform of E_z at Point C (at a depth of 12 m in the 0.001-S/m soil) in the absence of river, and Fig. 2 (c-2) shows that in the presence of river (at a depth of 2 m in the 0.1-S/m soil under the from the river water). It appears that E_z at a depth of 2 m in the (0.1-S/m) high conducting soil is much more attenuated than that at a depth of 12 m in the (0.001-S/m) low conducting soil.

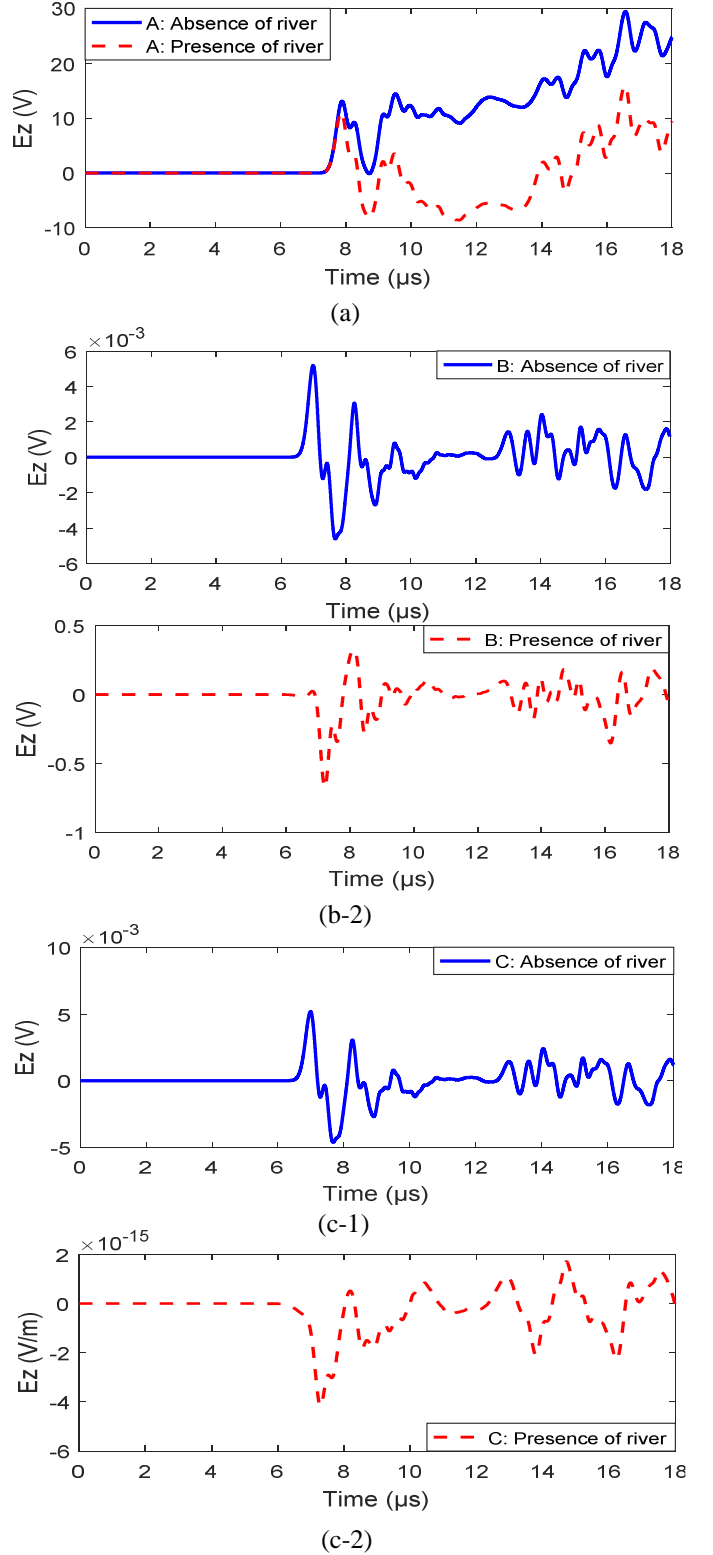


Fig. 2. Waveforms of vertical electric field E_z (a) at Point A in both the absence and presence of the river, (b-1) at Point B in the absence of river, (b-2) at Point B in the presence of river, (c-1) at Point C in the absence of river, and (c-2) at Point C in the presence of river.

B. Horizontal electric field

Space and time variations of the horizontal electric field E_y at Points A, B, and C in Fig. 1 are shown in this section. In order to show the influence of the presence of river, corresponding waveforms of E_y in the absence of river, where the 5-m deep and 0.005-S/m river, the 0.1-S/m high conducting soil layer below the river, and the 5-m thick air layer above the river are replaced by a uniform 0.001-S/m soil, are shown.

Fig. 3 (a) shows waveforms of E_y at Point A in both the presence and absence of river. It follows from Fig. 3 (a) that the presence of the 51-m wide and 5-m deep dip of the ground due to the river little influences E_y located beyond the river.

Fig. 3 (b-1) shows the waveform of E_y at Point B (at a depth of 7 m in the 0.001-S/m soil) in the absence of river, and Fig. 3 (b-2) shows that in the presence of river (at a depth of 2 m from the surface of 0.005-S/m river water). It appears that E_y at a depth of 7 m in the 0.001-S/m soil is much more attenuated than that at a depth of 2 m in the 0.005-S/m water although the waveforms are similar each other.

Fig. 3 (c-1) shows the waveform of E_y at Point C (at a depth of 12 m in the 0.001-S/m soil) in the absence of river, and Fig. 3 (c-2) shows that in the presence of river (at a depth of 2 m in the 0.1-S/m soil under the from the river water). It appears that E_y at a depth of 2 m in the (0.1-S/m) high conducting soil is much more attenuated than that at a depth of 12 m in the (0.001-S/m) low conducting soil although the waveforms are similar each other.

C. Azimuthal magnetic field

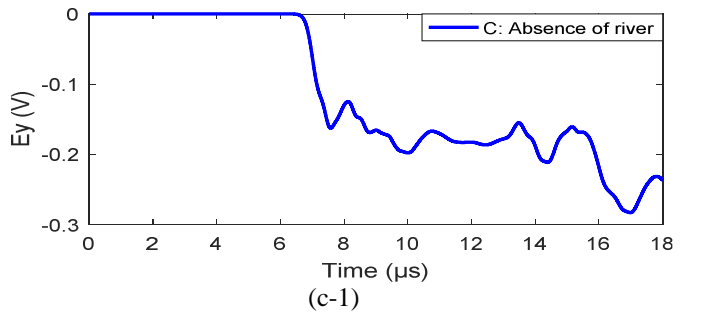
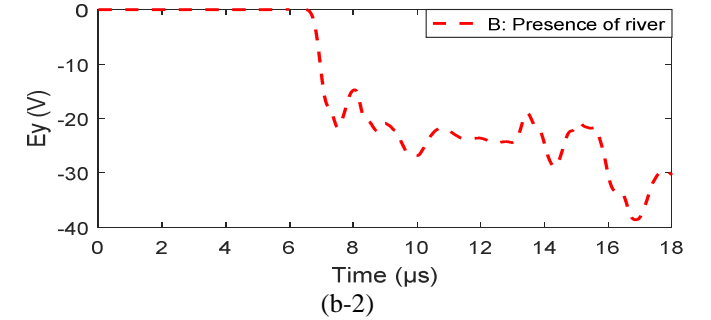
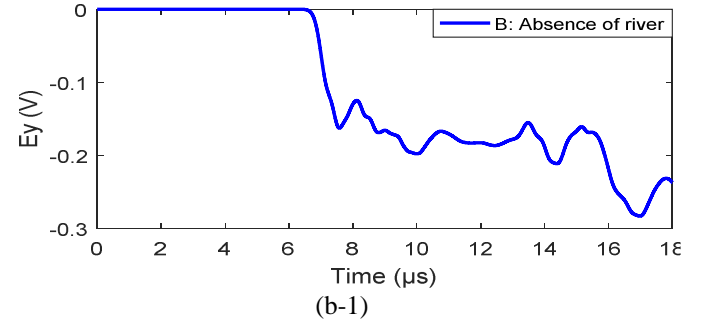
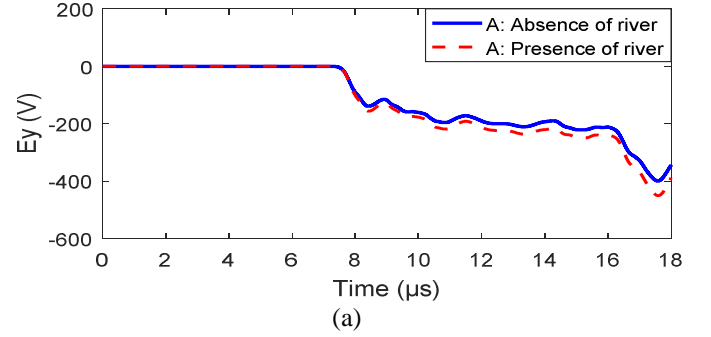
Space and time variations of the azimuthal magnetic field H_x at Points A, B, and C in Fig. 1 are shown in this section. In order to show the influence of the presence of river, corresponding waveforms of H_x in the absence of river, where the 5-m deep and 0.005-S/m river, the 0.1-S/m high conducting soil layer below the river, and the 5-m thick air layer above the river are replaced by a uniform 0.001-S/m soil, are shown.

Fig. 4 (a) shows waveforms of H_x at Point A in both the presence and absence of river. It follows from Fig. 4 (a) that the presence of the 51-m wide and 5-m deep dip of the ground due to the river decreases H_x (by 20 to 30%) located beyond the river.

Fig. 4 (b-1) shows the waveform of H_x at Point B (at a depth of 7 m in the 0.001-S/m soil) in the absence of river, and Fig. 4 (b-2) shows that in the presence of river (at a depth of 2 m from the surface of 0.005-S/m river water). It appears that H_x at a depth of 7 m in the 0.001-S/m soil is much more attenuated than that at a depth of 2 m in the 0.005-S/m water although the waveforms are similar each other.

Fig. 4 (c-1) shows the waveform of H_x at Point C (at a depth of 12 m in the 0.001-S/m soil) in the absence of river,

and Fig. 4 (c-2) shows that in the presence of river (at a depth of 2 m in the 0.1-S/m soil under the from the river water). It appears that H_x at a depth of 2 m in the (0.1-S/m) high conducting soil is much more attenuated than that at a depth of 12 m in the (0.001-S/m) low conducting soil although the waveforms are similar each other.



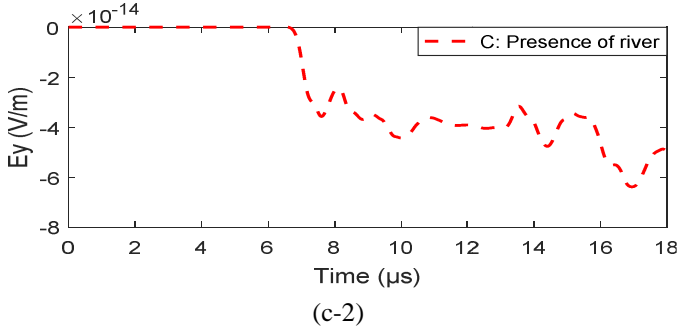


Fig. 3. Waveforms of horizontal electric field E_y (a) at Point A in both the absence and presence of the river, (b-1) at Point B in the absence of river, (b-2) at Point B in the presence of river, (c-1) at Point C in the absence of river, and (c-2) at Point C in the presence of river.

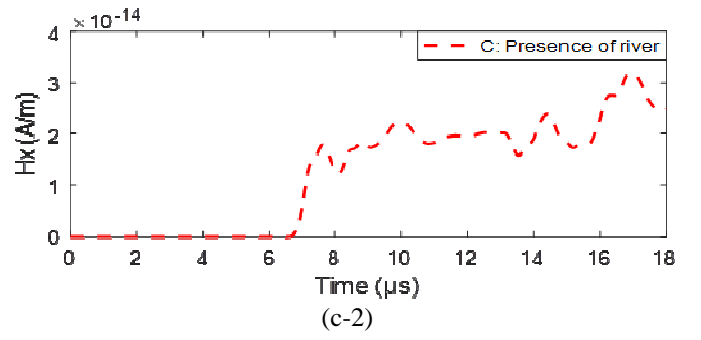


Fig. 4. Waveforms of azimuthal magnetic field H_x (a) at Point A in both the absence and presence of the river, (b-1) at Point B in the absence of river, (b-2) at Point B in the presence of river, (c-1) at Point C in the absence of river, and (c-2) at Point C in the presence of river.

IV. CONCLUSION

We have set ourselves in this paper as the main objective to examine the influence of the presence of a wide river on the amplitude and the waveforms of electromagnetic fields generated by lightning strikes on a high tower placed at the top of a high mountain. This study is justified by the fact that in practice we often encounter complex reliefs including mountains and streams (lakes, rivers,...) around which there are high towers (telecommunication towers for example) subject to lightning strikes generating radiated electromagnetic fields. These latter can couple with electrical lines or cables located in their close environment producing in these last overcurrents or overvoltages.

This study allowed us to show that the vertical electric field and the azimuthal magnetic field beyond the river are reduced by the presence of the river, while the horizontal (radial) electric field is slightly influenced. In addition, we have also highlighted that fields under the river are extremely small because of the shielding effect of the high conducting soil (0.1 S/m). Thus, magnitudes of fields in the river (2 m below the water surface of 0.005-S/m) are higher than corresponding fields in the soil (7 m below the ground surface of 0.001-S/m).

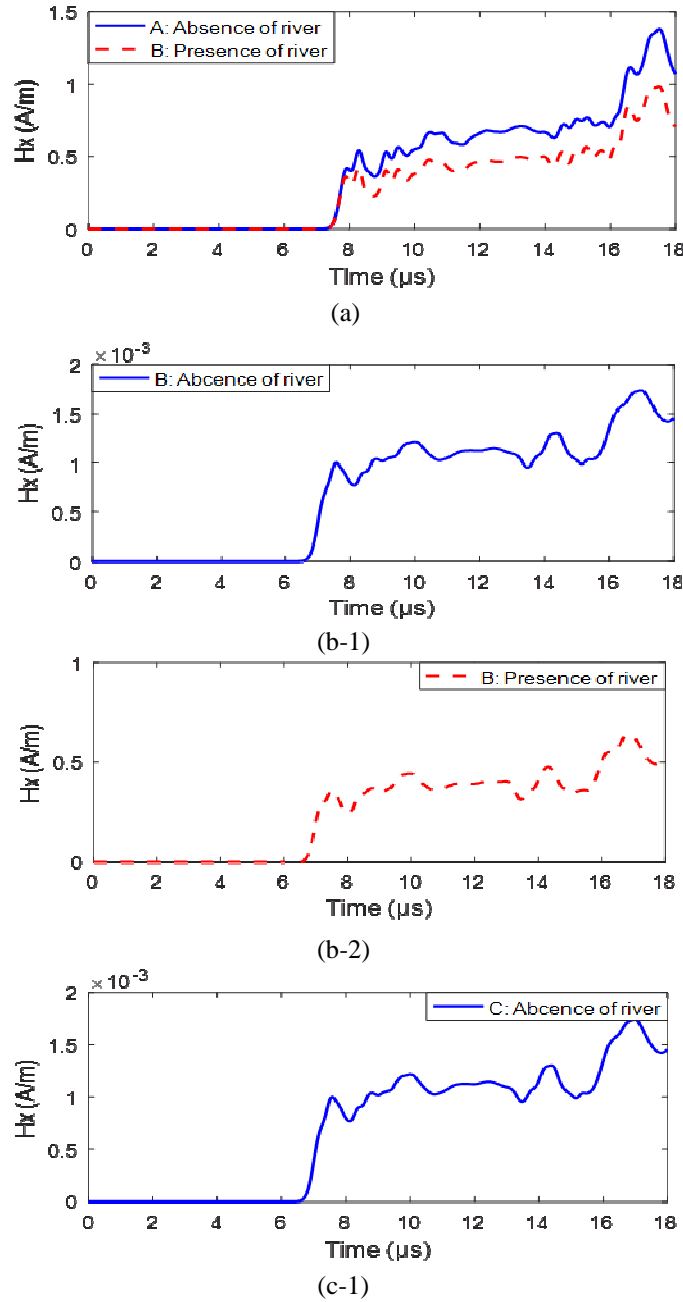
Finally, it should be noted that the calculated electromagnetic fields will make it possible to carry out coupling studies of these fields with overhead power lines or buried electric cables in order to determine overvoltages and overcurrents induced in these structures, which will allow, on the practical plan, to correctly size their protection against these indirect lighting effects.

ACKNOWLEDGMENT

Part of this study was carried out in the Power System Analysis Laboratory of Doshisha University, Japan. The authors would like to thank Prof. A. Ametani and Prof. N. Nagaoka for their kind cooperation.

REFERENCES

- [1] F. Rachidi, V. A. Rakov, C. A. Nucci, and J. L. Bermudez, "Effect of vertically extended strike object on the distribution of current along the lightning channel", *Journal of Geophysical Research*, Vol. 107, No. D23, 4699, 2002.



- [2] Y. Baba, and V. A. Rakov, "On the use of lumped sources in lightning return stroke models", *Journal of Geophysical Research*, Vol. 110, No. D3, D03101, doi:10.1029/2004JD005202, 2005.)
- [3] F. Rachidi, "Modeling lightning return strokes to tall structures: A review", *Journal of Lightning Research*, Vol. 1, pages 16–31, 2007.
- [4] Y. Baba, and M. Ishii, "Numerical electromagnetic field analysis of lightning current in tall structures", *IEEE Trans. Power Delivery*, Vol. 16, No. 2, April 2001.
- [5] Y. Baba and V. A. Rakov, "Lightning strikes to tall objects: Currents inferred from far electromagnetic fields versus directly measured currents", *Geophysical Research Letters*, Vol. 34, 2007.
- [6] Y. Baba, and V. A. Rakov, "Influence of strike object grounding on close lightning electric fields", *Journal of Geophysical Research*, Vol. 113, 2008.
- [7] Y. Baba, and V. A. Rakov, *Electromagnetic Computation Methods for Lightning Surge Protection Studies*, Wiley-IEEE Press, 2016.
- [8] J. L. Bermudez, F. Rachidi, M. Rubinstein, W. Janischewskyj, V. O. Shostak, D. Pavanello, J. S. Chang, A. M. Hussein, C. A. Nucci, and M. Paolone, "Far-field-current relationship based on the TL model for lightning return strokes to elevated strike objects", *IEEE Trans. Electromagnetic Compatibility*, Vol. 47, No. 1, Feb. 2005
- [9] J. L. Bermudez, M. Rubinstein, F. Rachidi, F. Heidler, and M. Paolone, "Determination of reflection coefficients at the top and bottom of elevated strike objects struck by lightning", *Journal of Geophysical Research*, Vol. 108, No. D14, 2003
- [10] D. Pavanello, F. Rachidi, M. Rubinstein, J. L. Bermudez, and C. A. Nucci, "Electromagnetic field radiated by lightning to tall towers: Treatment of the discontinuity at the return stroke wave front", *Journal of Geophysical Research*, Vol. 109, 2004
- [11] A. Mosaddaghi, D. Pavanello, F. Rachidi, and M. Rubinstein, "Electric and magnetic fields at very close range from the lightning strike to a tall object", 19th International Zurich Symposium on Electromagnetic Compatibility, P 8, Singapore, May 2008.
- [12] A. Mosaddeghi, A. Shoory, F. Rachidi, G. Diendorfer, H. Pichler, D. Pavanello, M. Rubinstein, P. Zwiack, and M. Nyffeler, "Lightning electromagnetic fields at very close distances associated with lightning strikes to the Gaisberg tower", *Journal of Geophysical Research*, Vol. 115, 2010.
- [13] A. Mosaddeghi, F. Rachidi, M. Rubinstein, F. Napolitano, D. Pavanello, V. O. Shostak, W. Janischewskyj, and M. Nyffeler, "Radiated Fields from lightning strikes to tall structures: Effect of upward-connecting leader and reflections at the return stroke wavefront", *IEEE Trans. Electromagnetic Compatibility*, Vol. 53, No 2, May 2011.
- [14] A. Shoory, F. Rachidi, and M. Rubinstein, "Relativistic doppler effect in an extending transmission line: Application to lightning", *Journal of Geophysical Research*, Vol. 116, 2011.
- [15] A. Shoory, F. Rachidi, and M. Rubinstein, "Correction to relativistic doppler effect in an extending transmission line: Application to lightning", *Journal of Geophysical Research*, Vol. 117, 2012.
- [16] R. Khosravi, S. H. Sadeghi and R. Moini, "Electromagnetic field due to lightning strikes to mountainous ground", *Amirkabir International Journal of Science & Research (Electrical & Electronics Engineering - AIJ-EEE)*, Vol. 47, No. 2, pp. 27- 37, 2015.
- [17] E. Soto, E. Perez, and J. Herrera, "Electromagnetic field due to lightning striking on top of cone-shaped mountain using FDTD", *IEEE Trans. Electromagnetic Compatibility*, Vol. 56, No. 5, pp. 1112-1120, Oct. 2014.
- [18] D. Li, M. Azadifar, F. Rachidi, M. Rubinstein, M. Paolone, D. Pavanello, S. Metz, Q. Zhang, and Z. Wang, "On lightning electromagnetic field propagation along an irregular terrain", *IEEE Trans. Electromagnetic Compatibility*, Vol. 58, No. 1, pp. 161-171, Feb. 2016.
- [19] D. Li, M. Azadifar, M. Rubinstein, F. Rachidi, G. Diendorfer, W. Schulz, and G. Lu, "Location accuracy evaluation of ToA-based lightning location systems over mountainous terrain", *Journal of Geophysical Research: Atmospheres*, Vol. 122.21 pp 760-775, 2017.
- [20] M. Azadifar, F. Rachidi, M. Rubinstein, M. Paolone, G. Diendorfer, H. Pichler, W. Schulz, D. Pavanello, and C. Romero, "Evaluation of the performance characteristics of the European lightning detection network EUCLID in the Alps region for upward negative flashes using direct measurements at the instrumented S ntis tower", *Journal of Geophysical Research: Atmospheres*, Vol. 121.2 pp 595-606, 2016.
- [21] K. Arzag, Z. Azzouz, Y. Baba and B. Ghemri "3-D FDTD computation of the electromagnetic fields associated with lightning strikes to a tower climbed on a trapezoidal mountain", *IEEE Trans. Electromagnetic Compatibility*, in press.
- [22] J. Paknahard, K. Sheshyekani, M. Hamzeh and F. Rachidi "Lightning induced currents on river-crossing buried cables", in *Proc. 2014. International Conference on Lightning Protection (ICLP)*, pp 581-584, Shanghai, China, Oct. 2014.
- [23] Y. Baba, and V. A. Rakov, "Application of the FDTD method to lightning electromagnetic pulse and surge simulation", *IEEE Trans. Electromagnetic Compatibility*, Vol. 56, No. 6, pp 1506-1521, Dec. 2014.
- [24] K. S. Yee, "Numerical solution of initial boundary value problems involving Maxwell's equations in isotropic media", *IEEE Trans. Antennas and Propagation*. Vol. AP-14, No. 3, pp 302-307, May, 1966.
- [25] R. F. Harrington, *Field Computation by Moment Methods*, New York: Macmillan, 1968.
- [26] M. N. O. Sadiku, "A simple introduction to finite element analysis of electromagnetic problems", *IEEE Trans. on Education*, Vol. 32, No. 2, pp. 85-93, 1989.
- [27] A. Taflov, and S. C. Hagness, *Computational electrodynamics: the finite-difference time-domain method*, Second Edition, Artech House, Boston-London, 2000.
- [28] K. Arzag, Z. Azzouz, and B. Ghemri, "Lightning electric and magnetic fields computation using the 3D-FDTD method and electromagnetic models in presence of different ground configurations", *IEEE Trans. Power and Energy*, Vol. 138, no. 5, pp. 315–320, May 2018.
- [29] K. Arzag, Z. Azzouz, Y. Baba, and B. Ghemri "3D computation of lightning electromagnetic fields in the presence of a horizontally stratified ground", *International Journal of Power and Energy Systems*, Vol. 37, No. 4, pp 120-128, Dec. 2017.
- [30] M. A. Uman, D. K. McLain, and E. P. Krider "The electromagnetic radiation from a finite antenna", *Amer. J. Phys.*, Vol. 43, pp. 33-38, 1975.
- [31] F. Heidler "Analytic lightning current functions for LEMP calculations", in *Proc. 1985. International Conference on Lightning Protection (ICLP)*, pp 63-66, Munich, Germany, Sep. 1985.